SPE-180072-MS

A New Non-Darcy Flow Model for Low Velocity Multiphase Flow in Tight Reservoirs

Yi Xiong, Colorado School of Mines; Jinbiao Yu, and Hongxia Sun, China Petroleum & Chemical Corp; Jiangru Yuan, RIPED of PetroChina; Zhaoqin Huang, China University of Petroleum; Yu-shu Wu, Colorado School of Mines

Copyright 2016, Society of Petroleum Engineers

This paper was prepared for presentation at the SPE Europec featured at 78th EAGE Conference and Exhibition held in Vienna, Austria, 30 May – 2 June 2016.

This paper was selected for presentation by an SPE program committee following review of information contained in an abstract submitted by the author(s). Contents of the paper have not been reviewed by the Society of Petroleum Engineers and are subject to correction by the author(s). The material does not necessarily reflect any position of the Society of Petroleum Engineers, its officers, or members. Electronic reproduction, distribution, or storage of any part of this paper without the written consent of the Society of Petroleum Engineers is prohibited. Permission to reproduce in print is restricted to an abstract of not more than 300 words; illustrations may not be copied. The abstract must contain conspicuous acknowledgment of SPE copyright.

Abstract

This paper is to present a new non-linear flow model for low-velocity multiphase flow in tight petroleum reservoirs as well as its analytical and numerical solutions. The pore and pore-throat sizes of shale and tight-rock formations are on the order of tens of nanometers. The fluid flow in such small pores is significantly affected by walls of pores and pore-throats. This boundary-layer effect on fluid flow in tight rocks has been investigated through laboratory work. In analogue to flow through capillary tubes, it is found that the ratio of the thickness of boundary layer over the size of capillary tube is a function of pressure gradient; and the non-linear relationship between flow rate and pressure gradient is pronounced under the drive of small pressure gradient or low flow velocity. It is also observed that low permeability is associated with large boundary layer effect on fluid flow. Based on the studies of single-phase and multiphase flow though capillary tubes, the new non-Darcy flow model is proposed for describing multiphase flow in tight rock.

The experimental results from a single capillary tube are extended to a bundle of tubes and finally to porous media of tight formations. A physics-based, non-Darcy low-velocity flow equation is derived to account for the boundary layer effect of tight reservoirs by adding a non-Darcy coefficient term, which is function of dimensionless thickness of boundary layer and pressure gradient. This non-Darcy equation describes the fluid flow more accurately for tight oil reservoir with low production rate and low pressure gradient as compared to laboratory observation.

Both analytical and numerical solutions are obtained for the new non-Darcy flow model. First, a Buckley-Leverett type analytical solution is derived including gravity effect with this non-Darcy flow equation. Then, a numerical model has been developed for implementing this non-Darcy flow model for accurate simulation of multi-dimensional porous and fractured tight oil reservoirs. The sensitivity studies based on numerical simulations demonstrate the non-negligible effect of boundary layer on fluid flow in tight formations using an actual field example. Eventually, the experiment-based non-Darcy flow model could improve the forecast accuracy for long-term production rate and recovery factors of tight oil reservoirs.

A new, physics-based low-velocity non-Darcy flow model is developed for description of single-phase and multiphase flow in tight reservoirs. In addition, both analytical and numerical solutions are provided for application of the new non-Darcy flow model for field studies. The results and knowledge obtained in this study may be applicable to both oil and gas flow in unconventional reservoirs.

Introduction

Darcy's law (Darcy, 1856) is the exclusive formulation to model subsurface fluid flow in oil and gas reservoirs, which describes a linear relationship between volumetric flow rate (Darcy velocity) and pressure gradient. It is also the fundamental principle for many other applications in oil and gas industry, especially, in the areas of well testing analysis and reservoir simulation (Ahmed and McKinney, 2011; Aziz and Settari, 1979). On the other hand, Darcy's law is only valid for laminar and viscous flow (Ahmed, 2006), and any deviations from this linear relation can be defined as non-Darcy flow. It has long been recognized that non-Darcy flow phenomena could exist in many systems involving high flow rate, e.g. shale gas reservoirs (Zhao et al., 2015a, 2015b), CO_2 sequestration, and Enhanced Oil Recovery (EOR) system (Zhang et al., 2013, 2015a, 2015b), and enhanced geothermal system (Wu, et al., 2014, Xiong et al., 2013). For example, Forchheimer (1901) extended Darcy's linear form to a quadratic flow equation, and eventually added an additional cubic term to formulate flow at high flow rate in porous media. In addition, many efforts have been added to improve Forchheimer model for fitting larger range of fluid flow with high flow rate (Carman, 1997; Ergun, 1952; Montillet, 2004) and extend it to multiphase conditions (Evan and Evan, 1988; Evan et. al., 1987). Barree and Conway (2004) proposed a new high velocity non-Darcy flow model based on experimental results and field observation. It is more general than Forchheimer model since it does not rely on the assumption of a constant permeability. Both of the two non-Darcy flow models have been widely applied to the numerical studies in oil and gas reservoirs (Wu, et al., 2010), CO_2 sequestration and EOR (Zhang et al., 2014) under high flow rate.

In addition to extensive investigations on high velocity non-Darcy flow, the non-linear relationship between volumetric flow rate and pressure gradient are also observed and studied for low-velocity fluid flows. For example, Prada and Civan (1999) introduce the concept of threshold pressure gradient to correct Darcy's law for low-velocity flow where fluids can flow through porous media only if the fluid flowing force is sufficient to overcome the threshold pressure gradient, and they recommend further research to improve correlations of the threshold pressure gradient. Gavin (2004) calls the departure from Darcy's law at low fluid velocities as "Pre-Darcy behavior" in petroleum reservoirs, and claims that there could be substantial unrecognized opportunities for increasing hydrocarbon recovery. Zeng et al. (2011) design experimental equipment to investigate single-phase flow in ultra-low permeability cores, using capillary flow meter to achieve accurate measurement of fluid volume. Their results confirm that the single-phase flow in ultra-low permeability cores is not consistent with Darcy's Law. Liu et al. (2015) propose a phenomenological model for non-Darcy liquid flow in shale and develop an analytical solution to one-dimensional spontaneous imbibition problem that obeys the model. In addition, the low-velocity non-Darcy phenomena are also intensively studied in non-petroleum disciplines. Hansbo (1960, 2001) report a power function between flux and pressure gradient for water flow in low-permeability clay soil under small values of pressure gradient, and become linear if pressure gradient becomes larger. Swartzendruber (1961) propose to modify the linear relationship of Darcy's law to an exponential function for water flow in tight soil. Liu (2014) indicate that non-Darcy flow behavior is common in low-permeability media through reviewing studies on water flow in shale formations under the context of nuclear waste disposal.

In this paper, we study non-Darcy flow in low permeability reservoir through experiments, theoretical analysis, and numerical simulation. The next section presents our experimental results from a single capillary tube, which shows the effect of a boundary layer of fluid in capillary tube on flow behavior. The results from a single capillary tube are then extended to multiple tubes and to multiphase flow in a porous medium. Our empirical formulation from experimental data is a continuous function including both Darcy and non-Darcy flows, and a numerical model has been developed to capture this experiment-based non-Darcy fluid behavior. Finally, we perform a field study with this numerical model for a multi-stage hydraulic fracturing well in a tight oil reservoir.

Experimental Results

The experiment is performed on a single capillary tube with radius r shown in Figure 1 (a), where the flow is divided into body flow and boundary flow, and the thickness of boundary flow is δ. The body flow is the fluid flow not affected by tube wall, and boundary flow is the portion of fluid under the effect of tube wall. The smaller of capillary tube, the larger of boundary flow relatively. Our experimental results show an exponential function between ratio of thickness of boundary flow over tube radius and pressure gradient, described in Equation (1).

$$\frac{\delta}{r} = \delta_D e^{-c\nabla p} \tag{1}$$

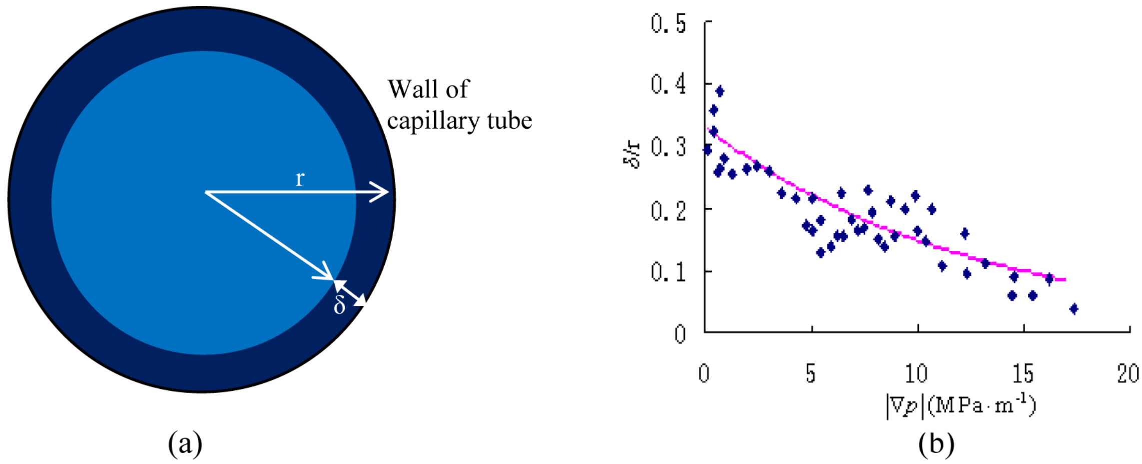

Figure 1—(a) Flow in capillary tube; (b) Relationship between ratio of thickness of boundary flow over tube radius and pressure gradient

In addition, we also found that there is a static boundary layer δ_0, which is independent from pressure gradient or flow velocity. And δ_D in Equation (1) is a dimensionless boundary layer, denoted as ratio of static boundary layer over tube radius, $\delta_D = \delta_0/r$. We also introduce a coefficient c, which is a regression parameter to match exponential function. The flow rate then can be derived from Equation (1) and Hagen-Poiseuille Equation as below.

$$q = \int_0^{r_0-\delta} v(r).2\pi r dr = \frac{\pi\left(1-\delta_D e^{-c|\nabla p|}\right)^4 r_0^4}{8\mu}|\nabla p| \tag{2}$$

The equation above is a linear function of Hagen-Poiseuille Equation between flow rate and pressure gradient if pressure gradient becomes large:

$$q = \frac{\pi r_0^4}{8\mu}|\nabla p| \tag{3}$$

Again, c and δ_D are two parameters determined from experiment results to match the non-linear relationship between flow rate and pressure gradient under the drive of a small pressure gradient. We performed an experiment in a capillary tube with 2.5 μm radius, and the results show a good agreement with Equation (2) with the determined c and δ_D values, shown in Figure 2 (a). Figure 2 (b) plots the extent of non-linearity with different c values. A smaller c value gives larger extent of non-linearity and an infinity value of c essentially gives a linear function.

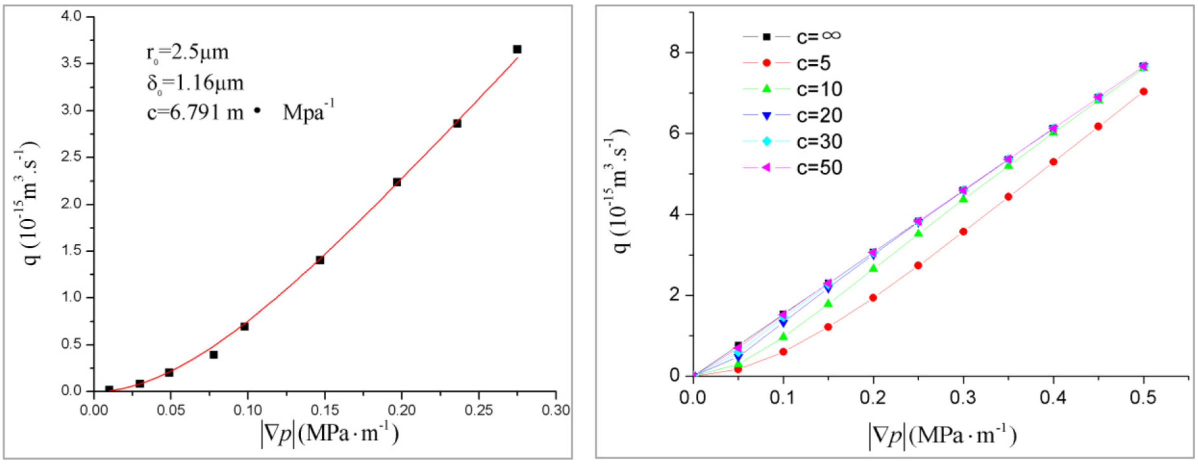

Figure 2—(a) Flow rate vs. pressure gradient from experimental results (b) The extent of non-linearity for different values of *c*

The single tube experiment-based non-linear function Equation (2) can be extended to flow through multiple tubes:

$$Q = \sum_{i=1}^{N} n_i q(r_i) = \sum_{i=1}^{N} n_i \frac{\pi\left(1-\delta_i e^{-c_i|\nabla p|}\right)^4 r_i^4}{8\mu}|\nabla p| \tag{4}$$

According to Hagen-Poiseuille Equation, the equavalent form of Equation (4) for a porous medium can be written as

$$v = \frac{k\left(1-\delta_D e^{-c_\phi|\nabla p|}\right)^4}{\mu}\nabla p \tag{5}$$

where k and μ are absolute permeability and fluid viscosity. Equation (5) is our experiment-based single phase non-Darcy flow model with non-Darcy terms, related to boundary flow. One big advantage of Equation (5) is that it is a continuous function describing both Darcy and non-Darcy flow with a single formulation, with more accuracy on low-velocity flow under small pressure gradient. Equation (5) can further extended to multiphase flow through two-phase experiments, which measure dimensionless boundary layer of each phase under a variety of permeability and water fractional flow. Table 1 summarizes the values of dimensionless boundary layer of each phase from two-phase experiments.

Table 1—Values of dimensionless boundary layer of water and oil phases

Permeability (mD)		δ_D of each phase at different water fractional flow f_w				Average δ_D
0.611		**f_w =0.877**	**f_w =0.768**	**f_w =0.644**	**f_w =0.456**	
	Water phase	0.348	0.374	0.372	0.389	0.37
	Oil phase	0.374	0.371	0.390	0.349	0.37
2.85		**f_w =0.942**	**f_w =0.905**	**f_w =0.855**	**f_w =0.724**	
	Water phase	0.291	0.319	0.403	0.352	0.34
	Oil phase	0.321	0.403	0.354	0.289	0.34
10.2		**f_w =1.0**	**f_w =0.805**	**f_w =1.712**	**f_w =1.624**	
	Water phase	0.115	0.118	0.188	0.123	0.14
	Oil phase	0.124	0.187	0.116	0.153	0.14

Table 1 show that δ_D could be different for different phase at the same water fractional flow, but the difference is quite small for low-permeability rock. On the other hand, the average values for oil and water phases are actually almost same. In addition, the lower permeability rock usually has a larger value of δ_D; it is because the lower permeability leads to a smaller flow portion of fluid and relative thicker static boundary layer. Therefore Equation (5) can have the multiphase version as Equation (6).

$$v_\beta = \frac{kk_{r\beta}\left(S_\beta\right)\left(1-\delta_D e^{-c_{\phi\beta}\left|\nabla p_\beta\right|}\right)^4}{\mu_\beta}\nabla p_\beta \tag{6}$$

where β can be either water or oil.

Numerical Model

A numerical model has been developed based on Equation (6) using an existing black oil reservoir simulator MSFLOW (Wu, 1998). The developed model can generally applied to tight oil reservoirs to study boundary layer induced non-Darcy effect. The numerical model is also validated against analytical solution for a Buckley-Leverett problem including gravity effect.

Validation of numerical model

A Buckley-Leverett problem including gravity effect is solved with the numerical model and an analytical solution, derived in this work. The rock and fluid parameters in Table 2 are used to get the fractional flow curve (analytical solution) and the numerical results. Table 3 lists the non-Darcy parameters in the validation example.

Table 2—Rock and fluid properties in the validation

Parameters	Values	Units
Absolute Permeability	1.0×10^{-14}	m^2
Porosity	0.1	
Residual Water Saturation	0.2	
Residual Oil Saturation	0.2	
Cross Section Area	1.0	m^2
Water Viscosity	1.139×10^{-3}	*Pa.s*
Water Density	1,000	kg/m^3
Oil Density	864	kg/m^3
Water Injection Rate	0.01728	m^3/day
Brooks-Corey k_r exponent	1.0	

Table 3—Non-Darcy parameters in the validation

Parameters	Water	Oil
δ_D	0.14	0.14
C_ϕ	10.1	2.1
Nonlinear exponent	4.0	4.0

The simulation domain is a 1D vertical rock column with 200 m by a uniform block-centered grid consisting of 100 elements. The water is injected at top and a constant pressure is described at 1 bar on the bottom boundary as Figure 3(a). With the input data in Table 1 and 2, a comparison of water saturation profiles at 100 days of injection, predicted by numerical code and analytical solution, is shown in Figure 3(b). The numerical and analytical results are in good agreement.

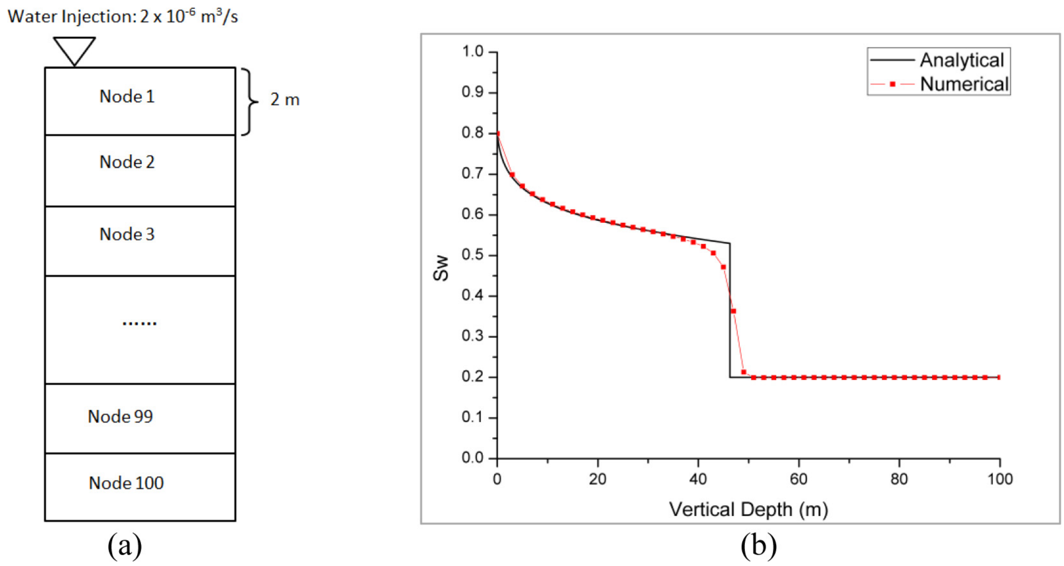

Figure 3—(a) Buckley-Leverett problem description (b) Numerical solution against analytical solution

Field Study

This section presents a field example studied with the developed numerical model, which mainly address a multi-stage hydraulic fractured well in a tight oil reservoir. In addition to non-Darcy flow, we also approximately include the geomechanical effect by including pore-pressure dependent porosity and transmissibility multiplier.

Reservoir and Well Description

The reservoir and well data are taken from a real tight oil reservoir in China with properties of rock and fluid shown in Table 4.

Table 4—Properties of rock and fluid in field study

Parameters	Values	Units
Absolute Permeability of matrix	1.0856×10^{-15}	m^2
Absolute Permeability of fracture	5.9215×10^{-12}	m^2
Porosity	0.149	
Residual Water Saturation	0.416	
Residual Oil Saturation	0.241	
Water Viscosity	0.45×10^{-3}	*Pa.s*
Water Compressibility	3.5×10^{-10}	Pa^{-1}
Water Density at STC	1000.0	$kg\ /\ m^3$
Oil Density at STC	872.4	$kg\ /\ m^3$
Initial Bubble-point Pressure	8.0	*MPa*
Initial Reservoir Pressure	32.21	*MPa*
Initial Oil Saturation	0.535	

The entire simulation is above bubble point pressure without gas phase. The water-oil two phase relative permeability and capillary pressure data shown in Table 5 are used for the simulation. As mentioned above, the porosity and transmissibility are functions of pore pressures. The correlations between multipliers and pore pressure shown in Table 6 are inputted to the simulation; and Table 7 lists the PVT properties used in the simulation. The non-Darcy flow parameters used in this field case are included in Table 8.

Table 5—Water-oil relative permeability and capillary pressure

S_w	K_{rw}	K_{ro}	P_{cow}(Pa)
0.416	0	1	5.57E+04
0.45	0.032	0.531	8.70E+03
0.485	0.063	0.26	8.00E+03
0.519	0.094	0.12	7.20E+03
0.553	0.127	0.06	6.50E+03
0.587	0.164	0.04	5.90E+03
0.622	0.207	0.022	5.00E+03
0.656	0.258	0.013	4.20E+03
0.69	0.318	0.006	3.40E+03
0.724	0.39	0.003	2.80E+03
0.759	0.475	0	2.40E+03

Table 6—Multipliers of porosity and transmissibility

Pore Pressure	Porosity Multiplier	Transmissibility Multiplier
1.00E+05	0.9031	0.01
7.00E+06	0.92656	0.105
1.47E+07	0.95274	0.335
1.97E+07	0.96974	0.381
2.37E+07	0.98334	0.451
2.61E+07	0.9915	0.504
2.77E+07	0.9955	0.584
2.97E+07	0.9975	0.681
3.12E+07	0.999	0.867
3.22E+07	1.000	1.00

Table 7—Reservoir PVT properties

Pressure (Pa)	Bo (rm3/stc-m3)	Rs (m3/m3)	Oil viscosity (Pa.s)
1.00E+05	1	0	1.78E-03
7.00E+06	1.215	55.462	1.68E-03
8.00E+06	1.246	63.5	1.58E-03
3.22E+07	1.231	63.5	1.88E-03
5.00E+07	1.22	63.5	2.11E-03

Table 8—Non-Darcy parameters

Parameters	Water	Oil
δ_D	0.35	0.35
c_ϕ	4.4	4.4
Nonlinear exponent	4.0	4.0

The simulation domain has a length of 1,894 m (x), width of 904 m (y) and thickness of 13 m (z), and divided into 104×47×5 with total number of 24,440 grid blocks. There are 12 stages hydraulic fractures for this horizontal well. The size of a general grid block is 20 m while the fracture node is 2 m. Figure 4 shows the mesh of simulation domain and Figure 5 demonstrates the lengths of 12 hydraulic fractures in x-y plane.

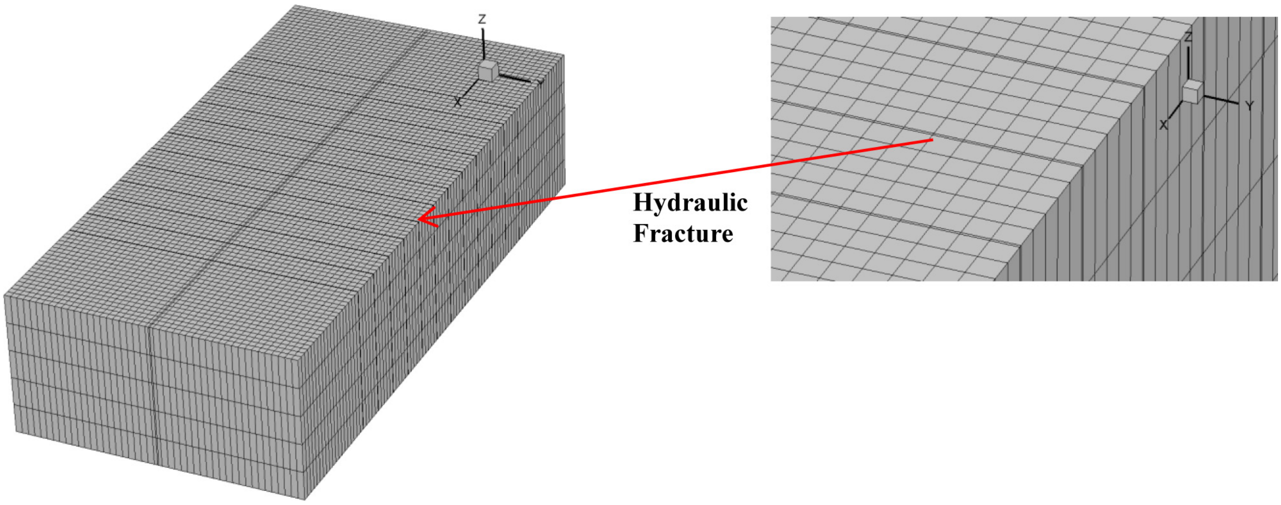

Figure 4—Grid blocks of simulation domain

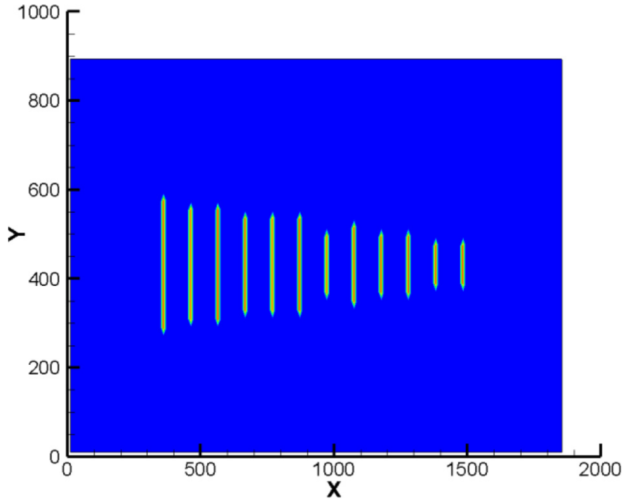

Figure 5—The length and shape of 12 stages of hydraulic fractures

Simulation Results and Discussion

With above reservoir properties and simulation input, the numerical model is ready to run by setting proper production mechanism. The production is controlled with constant wellbore pressure 8.2 MPa, which is above bubble point pressure 8.0 MPa, to maintain water and oil two phase flow production. Two simulation runs, Darcy fluid flow and non-Darcy fluid flow, are performed and compared to demonstrate the non-Darcy effect on the productions. Table 9 summarizes the comparison of critical values of the two simulation runs. The main difference is that Darcy model gives more accumulated production, because the non-Darcy coefficient reduces production rate. Accordingly non-Darcy model has higher reservoir pressure. Figure 6 to 9 presents the accumulated production and volumetric reservoir pressure throughout the simulation.

Table 9—Comparison of critical values after 70 years simulation

Values	Darcy Model	Non-Darcy Model
Initial gas volume (st-m3)	9.008×10^7	9.008×10^7
Initial water volume (st-m3)	1.531×10^6	1.531×10^6
Initial oil volume (st-m3)	1.419×10^6	1.419×10^6
Accumulated gas production (st-m3)	8.435×10^6	8.035×10^6
Accumulated water production (st-m3)	8.517×10^4	8.124×10^4
Accumulated oil production (st-m3)	1.328×10^5	1.265×10^5
Volumetric average reservoir pressure (MPa)	8.971	9.921
Volumetric average water saturation	0.4744	0.4738
Volumetric average oil saturation	0.5256	0.5262

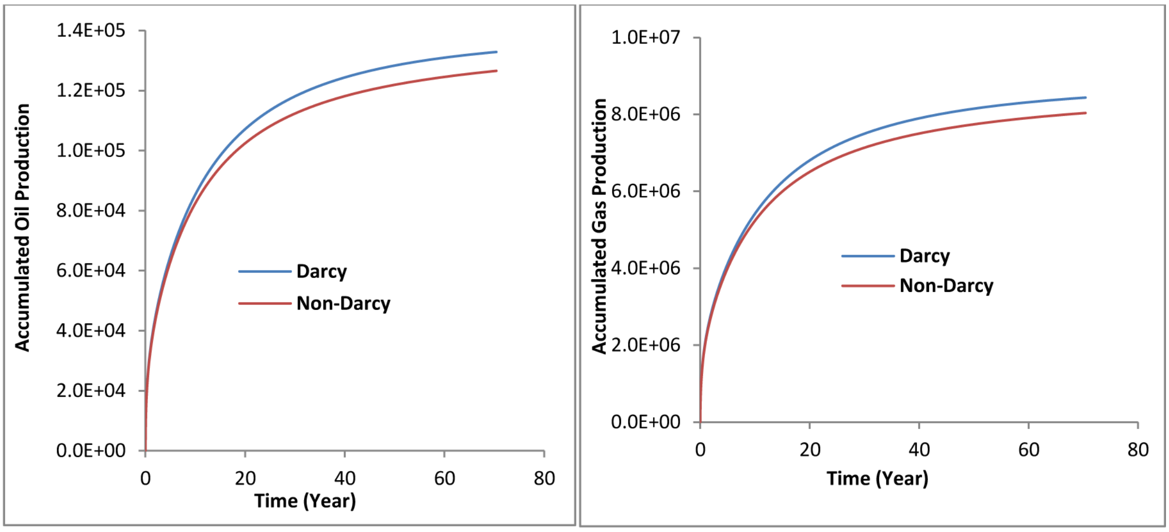

Figure 6—Comparison of accumulated oil and gas production

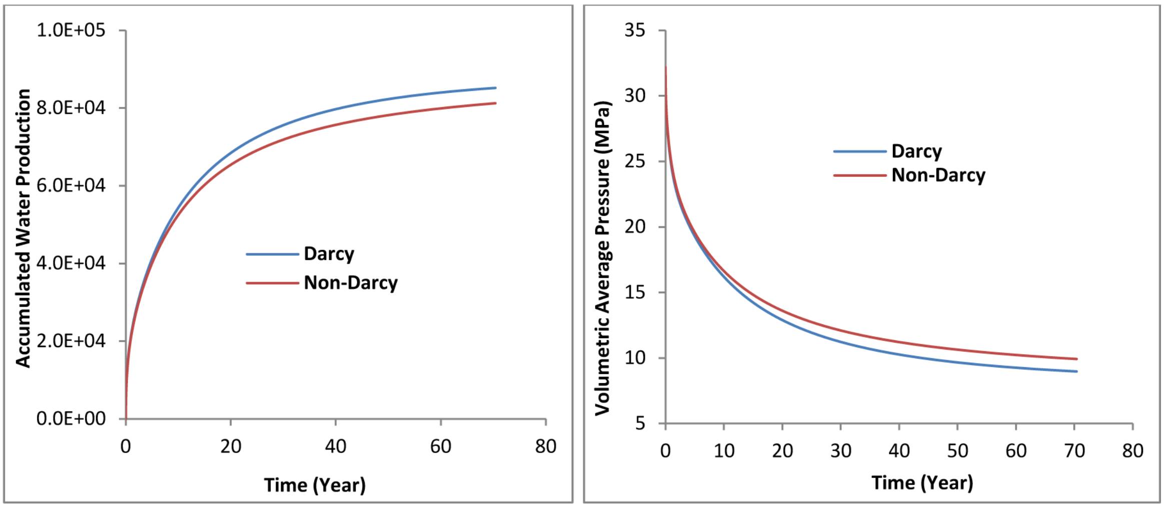

Figure 7—Comparison of accumulated water production and reservoir pressure

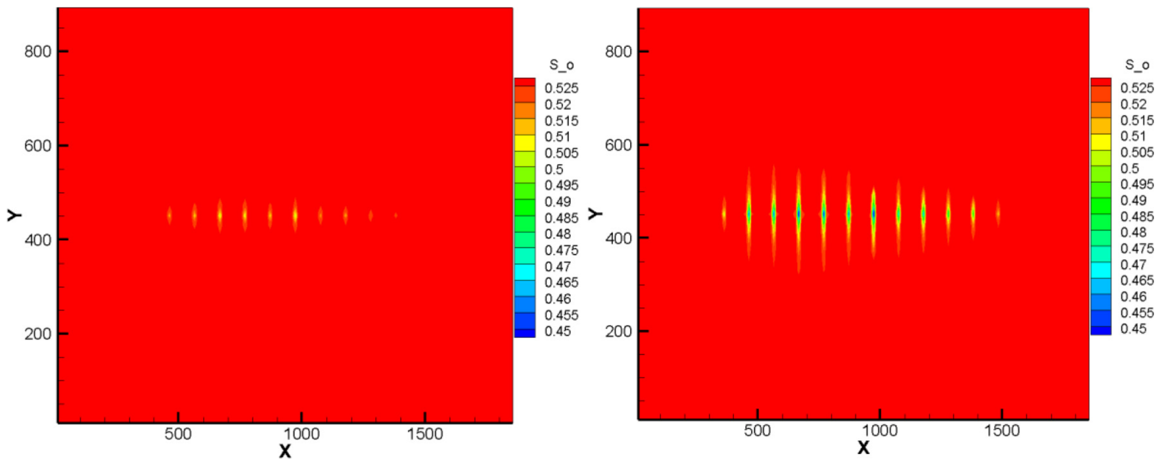

Figure 8—Oil Saturation of Non-Darcy flow model (left) and Darcy flow model (right)

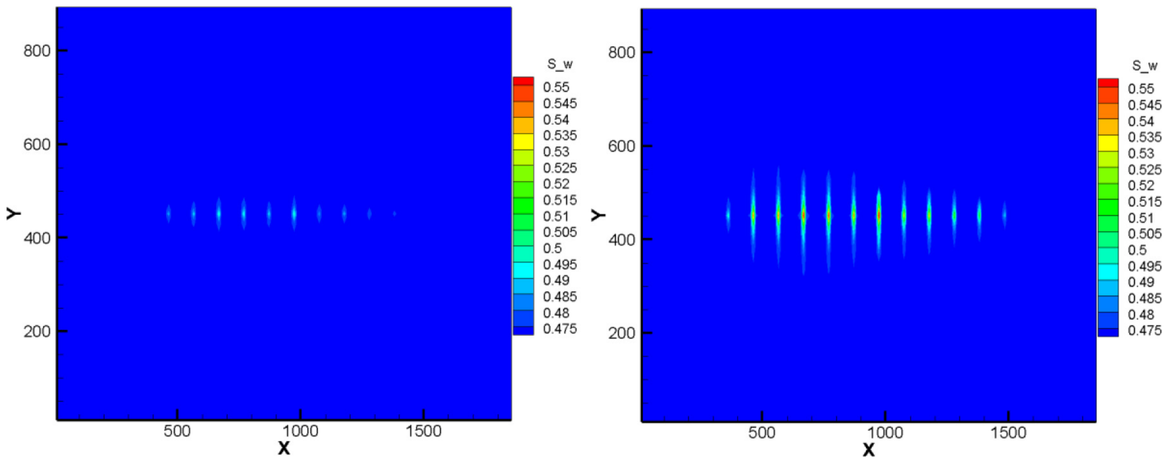

Figure 9—Water Saturation of Non-Darcy flow model (left) and Darcy flow model (right)

From Figure 6 to 9, it is shown that the simulation results of the two models overlap at the beginning because the non-Darcy flow model is equivalent with Darcy flow at high pressure gradient. After about 10 years' simulation, the non-Darcy flow presents different behaviors from Darcy flow due to larger value of non-Darcy coefficient at low pressure gradient. In other words, the low-velocity non-Darcy effect is non-negligible at the middle and end phases of field production, when the pressure gradient becomes small.

Figure 8 to 10 presents a variety of comparisons of contour diagram under Darcy and non-Darcy fluid flow at the end of 70 year production. Although the water and oil saturations are very close in the two models, the saturation close to the fractures shows larger differences that Darcy model has much lower oil saturation and higher water saturation; this is because the areas close to hydraulic fractures have small pressure gradient and therefore shows larger non-Darcy effect. The reservoir pressure, shown in Figure 13, has similar pattern in the two models. The pressure close to fractures is much lower than other areas, and the non-Darcy model shows a general higher reservoir pressure than Darcy model.

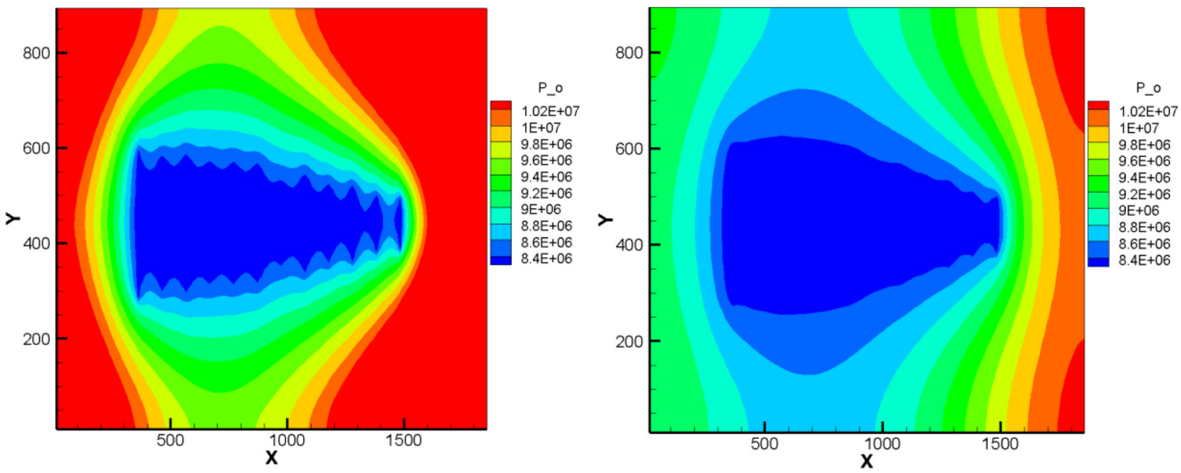

Figure 10—Reservoir Pressure of Non-Darcy flow model (left) and Darcy flow model (right)

This field example has reservoir permeability at 1.1 mD; we expect a much higher non-Darcy effect in tighter oil reservoirs. For example, three major tight formations in U.S. Bakken, Eagle Ford and Permian, usually have matrix permeability ranging from 10^{-5} md to 10^{-3} md (Xiong et al., 2015; Wang et al., 2015; Xiong 2015); therefore non-Darcy effect, induced by boundary layer of flow, could be much larger than the field study example above.

Conclusions

This paper presents an experiment-based non-Darcy fluid model for low-velocity flow in tight rock reservoirs. We observe a pressure gradient dependent boundary layer for the flow in a small capillary tube, further derive a single phase non-Darcy flow equation with two non-linear parameters, coefficient c and dimensionless boundary of flow $\boldsymbol{\delta_D}$. In addition, we analyze the non-Darcy effect for multiphase flow and performed an experimental study, which shows the phase-independent $\boldsymbol{\delta_D}$. Our multiphase non-Darcy equation provides a single formulation describing both Darcy and non-Darcy behaviors, where non-Darcy flow is only noticeable at a small pressure gradient.

This non-Darcy flow model has been successfully incorporated into a mature black oil reservoir simulator, MSFLOW, and the numerical implementation is verified with analytical solution. A real field study is then performed with the developed numerical model and the following conclusions are reached:

- The non-Darcy flow model has same simulation results as Darcy flow at the early part of simulation due to negligible non-Darcy coefficient under large pressure gradient. On the other hand, the non-Darcy flow behaviors are more obvious at the end of simulation due to large non-Darcy coefficients under low pressure gradient.
- The Darcy flow model gives about 5% larger accumulated production of oil and gas while non-Darcy flow model has about 10% higher reservoir pressure at end of 70 years' simulation for the reservoir with 1.1 mD permeability. We expect a much larger non-Darcy effect on production for a typical tight oil reservoir in U.S. with matrix permeability at 10^{-5} to 10^{-3} mD.
- A larger decrease in transmissibility occurs in Darcy than in non-Darcy flow due to 10% lower reservoir pressure. Thus Darcy flow could present higher accumulated production than the simulated results if there is no geomechanical (transmissibility multiplier) effect included.
- The field exmpale shows that two-phase production accounts for only 10% recovery; three-phase simulation is required to study the ultimate recovery. Therefore further study on boundary-induced non-Darcy effect is recommended for three phase coexisting fluid system.

Acknowledgement

This work was supported by the Foundation CMG, the EMG of the Colorado School of Mines, and by Geological Research Institute of SINOPEC Shengli Oilfield Company.

References

Ahmed, Tarek. Reservoir engineering handbook. *Gulf Professional Publishing,* 2006.

Ahmed, Tarek, and Paul McKinney. Advanced reservoir engineering. *Gulf Professional Publishing,* 2011.

Aziz, Khalid, and Antonin Settari. Petroleum reservoir simulation. *Chapman & Hall,* 1979.

Carman, P. C. ″Fluid flow through granular beds″. *Chemical Engineering Research and Design* **75** (1997): S32–S48.

Barree, R. D., and M. W. Conway. ″Beyond beta factors: a complete model for Darcy, Forchheimer, and trans-Forchheimer flow in porous media″. In SPE Annual Technical Conference and Exhibition. Society of Petroleum Engineers, 2004.

Buckley, S. E., and MC Leverett. ″Mechanism of fluid displacement in sands″. *Transactions of the AIME 146,* no. 01 (1942): 107–116.

Darcy, Henry. Les Fontaines Publiques de la Ville de Dijon, Dalmont, Paris. 1856

Ergun, Sabri. ″Fluid flow through packed columns″. *Chemical engineering progress* **48** (1952).

Evans, R. D., C. S. Hudson, and J. E. Greenlee. ″The effect of an immobile liquid saturation on the non-Darcy flow coefficient in porous media″. *SPE Production Engineering 2,* no. 04 (1987): 331–338.

Evans, E. V., and R. D. Evans. Influence of an Immobile or Mobile Saturation on Non-Darcy Compressible Flow of Real Gases in Propped Fractures. *JPT* **40** (10): 1343–1351. SPE-15066-PA. 10.2118/15066-PA, 1988.

Forchheimer, Philipp. ″Wasserbewegung durch boden″. *Z. Ver. Deutsch. Ing* **45,** no. 1782 (1901): 1788.

Gavin, Longmuir. ″Pre-Darcy flow: a missing piece of the improved oil recovery puzzle?″. In SPE/DOE Symposium on Improved Oil Recovery. Society of Petroleum Engineers, 2004.

Liu, Hui-Hai. ″Non-Darcian flow in low-permeability media: key issues related to geological disposal of high-level nuclear waste in shale formations″. *Hydrogeology Journal* **22,** no. 7 (2014): 1525–1534.

Liu, Hui-Hai, Bitao Lai, and Jinhong Chen. ″Unconventional Spontaneous Imbibition into Shale Matrix: Theory and a Methodology to Determine Relevant Parameters″. *Transport in Porous Media* **111,** no. 1 (2016): 41–57.

Montillet, Agne`s. ″Flow through a finite packed bed of spheres: a note on the limit of applicability of the Forchheimer-type equation″. *Journal of fluids engineering* **126,** no. 1 (2004): 139–143.

Prada, Alvaro, and Faruk Civan. ″Modification of Darcy's law for the threshold pressure gradient″. *Journal of Petroleum Science and Engineering* **22,** no. 4 (1999): 237–240.

Wang, Cong, Yu-Shu Wu, Yi Xiong, Philip H. Winterfeld, and Zhaoqin Huang. ″Geomechanics Coupling Simulation of Fracture Closure and Its Influence on Gas Production in Shale Gas Reservoirs″. *In SPE Reservoir Simulation Symposium. Society of Petroleum Engineers,* 2015.

Wu, Y. S. ″MSFLOW: Multiphase Subsurface Flow Model of Oil, Gas and Water in Porous and Fractured Media with Water Shut-off Capability, DOCUMENTATION and User's Guide″. (1998).

Wu, Yu-Shu., Zizhong Chen, Hossein Kazemi, Xiaolong Yin, Karsten Pruess, Curtis Oldenburg, Philip Winterfeld, Ronglei Zhang. ″Simulation of Coupled Processes of Flow, Transport, and Storage of CO2 in Saline Aquifers″, *Tech. rep., Trustees of The Colorado School of Mines,* 2014.

Wu, Yu-Shu, Perapon Fakcharoenphol, Ronglei Zhang. ″Non-Darcy Displacement in Linear Composite and Radial Flow Porous Media″, in *SPE EUROPEC/EAGE Annual Conference and Exhibition, Society of Petroleum Engineers,* 2010.

Xiong, Yi, Perapon Fakcharoenphol, Philip Winterfeld, Ronglei Zhang, and Yu-Shu Wu. ″Coupled Geomechanical and Reactive Geochemical Model for Fluid and Heat Flow: Application for Enhanced Geothermal Reservoir″, in SPE Reservoir Characterization and Simulation Conference and Exhibition, 16–18 September, SPE, Abu Dhabi, UAE, 2013.

Xiong, Yi, Philip Winterfeld, Cong Wang, Yu-shu Wu, and Zhaoqin Huang. ″A Compositional Model Fully Coupled with Geomechanics for Liquid-Rich Shale and Tight Oil Reservoir Simulation″. *In SPE Reservoir Simulation Symposium. Society of Petroleum Engineers,* 2015.

Xiong, Yi. ″Development of a compositional model fully coupled with geomechanics and its application to tight oil reservoir simulation″. *PhD dissertation, Colorado School of Mines,* 2015.

Zeng, Baoquan, Linsong Cheng, and Chunlan Li. ″Low velocity non-linear flow in ultra-low permeability reservoir″. *Journal of Petroleum Science and Engineering* **80,** no. 1 (2011): 1–6.

Zhang, Ronglei. ″Numerical Simulation of Thermal Hydrological Mechanical Chemical Processes during CO2 Geological Sequestration″, *PhD thesis, Colorado School of Mines,* 2013.

Zhang, Ronglei, Wu, Y-S. and Fakcharoenphol, P. (2014) ″Non-Darcy displacement in linear composite and radial aquifer during CO2 sequestration″, *International Journal of Oil, Gas and Coal Technology,* Vol. **7,** No. 3, pp.244–262.

Zhang, Ronglei, Philip H. Winterfeld, Xiaolong Yin, Yi Xiong, and Yu-Shu Wu. ″Sequentially Coupled THMC Model for CO2 Geological Sequestration into a 2D Heterogeneous Saline Aquifer″, *Journal of Natural Gas Science and Engineering,* Vol. **27,** pp.579–615, 2015a.

Zhang, Ronglei, Yi Xiong, Philip H. Winterfeld, Xiaolong Yin, and Yu-Shu Wu. ″A Novel Computational Framework for Thermal-Hydrological-Mechanical-Chemical Processes of CO2 Geological Sequestration into a Layered Saline Aquifer and a Naturally Fractured Enhanced Geothermal System', Greenhouse Gases: Science and Technology″ [online] 24 December 2015, in press, Accepted Manuscript, 2015b.

Zhao, Xiaoliang., Zhenhua Rui, Xinwei Liao, and Ronglei Zhang. ″The Qualitative and Quantitative Fracture Evaluation Methodology in Shale Gas Reservoir″, *Journal of Natural Gas Science and Engineering,* Vol. **27,** pp.486–495, 2015a.

Zhao, Xiaoliang., Zhenhua Rui, Xinwei Liao, and Ronglei Zhang. ″A Simulation Method for Modified Isochronal Well Testing to Determine Shale Gas Well Productivity″, *Journal of Natural Gas Science and Engineering,* Vol. **27,** pp.479–485, 2015b.